A Simplified procedure to assess the dynamic pressures on large reservoirs

L. Buldgen[1], H. Degée[2], H. Le Sourne[3], P. Rigo[2]

[1] FRIA PhD Student, Department of Structural Engineering, Faculty of Applied Sciences, University of Liège, Chemin des Chevreuils 1, 4000 Liège, Belgium

[2] Department of Structural Engineering, Faculty of Applied Sciences, University of Liège, Chemin des Chevreuils 1, 4000 Liège, Belgium

[3] Institut Catholique d'Arts et Métiers (ICAM), Avenue du Champ de Manoeuvres 35, 44470 Carquefou, France

Emails: L.Buldgen@ulg.ac.be, h.degee@ulg.ac.be, herve.lesourne@icam.fr, ph.rigo@ulg.ac.be

ABSTRACT: The paper is concerned with the seismic analysis of large reservoirs. During an earthquake, it is known that the acceleration of the water contained in the reservoir produces an additional hydrodynamic pressure, which has a convective, a rigid and a flexible impulsive part. The two first contributions are already well-known and may therefore be easily integrated during a pre-design phase, but it is much more complicated to assess the flexible contribution, as it is influenced by the coupling between the structure and the fluid. The only consistent way seems to resort to finite elements methods, which are not always convenient at an early design stage. For this reason, some research have been undertaken to rapidly evaluate the flexible pressure acting on thick plates. The results obtained by using this simplified method have been compared to numerical solutions. The agreement was found to be quite satisfactory.

KEY WORDS: Dynamic pressure; Seismic structural response; Modal analysis; Fluid structure interaction.

1 INTRODUCTION

When a reservoir is submitted to an earthquake, it is well known that an additional hydrodynamic pressure is applied on the tank walls, because of the acceleration of the water that is confined in the chamber. This pressure has the three following contributions:

- The convective one, which is produced by the waves occurring at the free surface during the seismic excitation. This phenomenon is also called sloshing.
- The rigid impulsive one, which is derived under the assumption that the walls are perfectly rigid and move in unison with the ground.
- The flexible impulsive one, coming from the accelerations of the walls as an imperfectly rigid structures.

The two first parts may be easily characterized by some analytical formulae already available in the literature. Many solutions were proposed by various authors, such as Epstein [1], Haroun [2], Housner [3] or Ibrahim [4] amongst others. It is therefore quite easy to account for these forces when designing new gates. Moreover, as we are presently dealing with quite large reservoirs, the convective part is negligible in comparison with the two remaining ones, so it will not be considered any longer in this study.

Assessing the third contribution is a more arduous task. In fact, the pressure field is influenced by the proper accelerations of the walls, which, in turn, has an effect on the dynamic response of the structure itself. In other words, we are facing a coupled problem. This one may be solved by resorting to finite elements analyses, where both the fluid and the structure have to be modeled. However, such an approach may be time demanding, because developing a complete and consistent numerical representation of the liquid is not so

easy. Moreover, modeling entirely the fluid domain may lead to excessively long calculation times. Of course, this way of working is definitely not acceptable at an early stage of design, when engineers do not necessarily have a lot of time to perform fastidious calculations. Such an approach is also not conceivable when a great amount of scenarios or configurations have to be checked.

For all these reasons, it is quite clear that an alternative approach is necessary, as integrating the seismic action in the pre-design is of prior importance in regions frequently submitted to earthquakes. Nevertheless, developing an efficient simplified analytical procedure is not so easy, but we propose to go one step further in this paper by considering a large flexible reservoir undergoing a seismic acceleration.
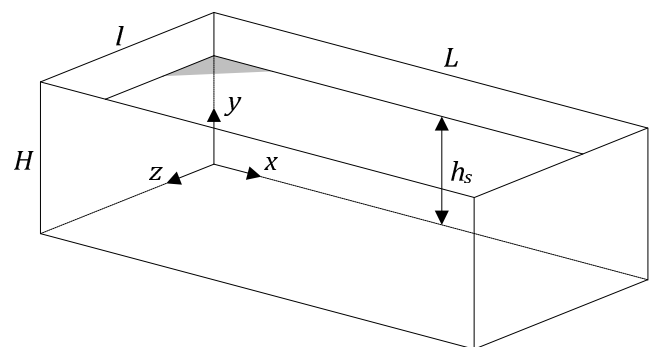

Figure 1. Flexible reservoir.

The tank under consideration here is depicted on Figure 1. It has a total length L, a width l and a height H. It is filled with water until the level h_s and is submitted to a longitudinal acceleration $\ddot{X}(t)$ acting along the x axis. The lateral walls located in $z = 0$ and $z = l$ are considered to be perfectly rigid.

This is also the case for the ground located at $y = 0$. On the contrary, the walls at $x = 0$ and $x = L$ are assumed to behave like a flexible plate simply supported on three edges (SS) and free at the upper one (F), as represented on Figure 2.

Figure 2. Boundary conditions.

2 FREE VIBRATION ANALYSIS OF A DRY PLATE

In this section, we consider the free vibrations of the isotropic and homogenous plate depicted on Figure 2. The plate is made of a linear elastic material characterized by a density ρ, a Young modulus E and a Poisson ratio v. The out-of-plane displacements along the x axis are denoted by $u(y,z,t)$.

Under the hypothesis of small strains, one may apply the classical thin plates theory of Kirchhoff, in which the structural equilibrium may be expressed as:

$$\rho t_p \left(\ddot{X} + \ddot{u} \right) + D \left(\frac{\partial^4 u}{\partial y^4} + 2 \frac{\partial^4 u}{\partial y^2 \partial z^2} + \frac{\partial^4 u}{\partial z^4} \right) = -p \tag{1}$$

$$\Leftrightarrow \rho t_p \left(\ddot{X} + \ddot{u} \right) + D \nabla^4 u = -p$$

where t_p and D are respectively the thickness and flexural rigidity of the plate. In equation (1), p denotes the total hydrodynamic pressure applied on the structure.

In order to derive the vibration properties for the dry plate, one can consider the homogenous form of equation (1), in which p and $\ddot{X}$ are set to zero. In this case, the proper displacements have a sinusoidal form:

$$u_i(y,z,t) = \delta_i(y,z) \sin(\omega_i t) \quad i \geq 1 \tag{2}$$

in which ω_i and δ_i are known as the dry eigenfrequencies and mode shapes. Introducing (2) in (1) and applying the developments of Leissa [5] leads to:

$$\left(\frac{\gamma_i^2(1-v) - c_i^2}{\gamma_i^2(1-v) + c_i^2} \right)^2 \overline{\lambda}_i \tan(\lambda_i H) - \lambda_i \tanh(\overline{\lambda}_i H) = 0 \tag{3}$$

where c_i is a function of ω_i that has to be determined by solving (3). All the other parameters are defined hereafter:

$$\overline{\lambda}_i^2 = c_i^2 + \gamma_i^2 \quad \lambda_i^2 = c_i^2 - \gamma_i^2 \quad \gamma_i = \frac{n_i \pi}{l} \quad c_i^4 = \frac{\rho \omega_i^2 t_p}{D} \tag{4}$$

with $n_i = 1, 2, \ldots$ Furthermore, as shown by [5], the dry mode shapes δ_i are given by:

$$\delta_i(y,z) = A_i \left(\sin\left(\frac{\lambda_i y}{l} \right) - B_i \sinh\left(\frac{\overline{\lambda}_i y}{l} \right) \right) \sin(\gamma_i z) \tag{5}$$

where A_i is the modal amplitude and B_i is related to the other variables by:

$$B_i = \frac{\gamma_i^2(1-v) - c_i^2}{\gamma_i^2(1-v) + c_i^2} \frac{\sin(\lambda_i H)}{\sinh(\overline{\lambda}_i H)} \tag{6}$$

It is worth bearing in mind that all the solutions detailed here above are only valid for a dry plate that is not in contact with water. In the present case however, the reservoir is filled up to a level h_s, which means that equations (3) and (5) are not the vibration properties characterizing the wet plate. To account for the presence of a fluid, we first need to have a better characterization of the hydrodynamic pressure term p appearing in equation (1).

3 FREE VIBRATION ANALYSIS OF A WET PLATE

3.1 Characterization of the hydrodynamic pressure

As recalled previously, a lot of analytical solutions are already available in the literature to evaluate the rigid impulsive pressure p_r. One may consider, amongst others, the expression proposed by Kim et al. [6]:

$$p_r = -\rho_f \left(\sum_{n=1}^{+\infty} \frac{4}{\beta_n^2 L} \frac{\cosh(\beta_n y)}{\cosh(\beta_n h_s)} - \frac{L}{2} \right) \cdot \ddot{X} \tag{7}$$

where $\beta_n = (2n - 1)\pi/L$ and ρ_f is the density of the fluid. On the other hand, if we still use the developments described by Rajalingham [7], the flexible impulsive contribution p_f can be derived from:

$$p_f = -\sum_{n=1}^{+\infty} \sum_{m=0}^{+\infty} C_{mn} \int_0^{h_s} \int_0^l \ddot{u} \cdot \cos(\alpha_n y) \cos(\kappa_m z) \cdot dy dz \tag{8}$$

in which $\alpha_n = (2n - 1)\pi/2h_s$ and $\kappa_m = m\pi/L$. The coefficient C_{mn} is expressed as:

$$C_{mn} = 2\rho_f \frac{1 - \cosh(\xi_{mn} L)}{\xi_{mn} h_s l_m \sinh(\xi_{mn} L)} \cos(\alpha_n y) \cos(\kappa_m z) \tag{9}$$

with $l_m = l$ if $m = 0$ and $l_m = l/2$ if $m > 0$. Equations (7) and (8) show that the rigid impulsive term p_r is not dependant from the proper displacements u of the wall, while it is not the case for the flexible part p_f. This means that the fluid-structure coupling is directly coming from p_f and not from p_r.

3.2 Vibration properties of a wet plate

As a second step, we may try to derive the vibration properties of a plate surrounded by water on one side. To do so, we consider the free vibrations problem by taking $\ddot{X} = 0$ in equation (1). This time however, as the plate is in contact with a fluid, the homogenous form of (1) is no longer valid. Indeed, to express the structural equilibrium, we have to account for the flexible pressure produced by the vibrations of the immerged plate. In other words, if we denote by Ω_i and Δ_i the wet eigenfrequencies and mode shapes, the proper displacements for such a situation may still be written in a similar manner than (2):

$$u_i(y,z,t) = \Delta_i(y,z) \sin(\Omega_i t) \quad i \geq 1 \tag{10}$$

but the characteristic equation to be solved for getting the modal properties is more difficult, as introducing (10) in (1) and (8) leads to:

$$\Omega_i^2\left(\rho t_p \Delta_i - \sum_{n=1}^{+\infty}\sum_{m=0}^{+\infty}C_{mn}I_{mn}\right) - D\nabla^4\Delta_i = 0 \qquad (11)$$

where I_{mn} is a term coming from the flexible pressure (8) and related to Δ_i by:

$$I_{mn}^{(i)} = \int_0^{h_s}\int_0^l \Delta_i \cdot \cos(\alpha_n y)\cos(\kappa_m z)\cdot dydz \qquad (12)$$

It is clear that finding an exact expression for Δ_i that satisfies (11) is almost impossible. An approximate analytical solution may however be found by applying the Rayleigh-Ritz method.

3.3 The Rayleigh-Ritz method

If we want to follow this approach, we first need to express Δ_i as a linear combination of admissible predefined functions that satisfy the boundary conditions detailed on Figure 2. As suggested by Rajalingham [7], we can directly use the dry mode shapes (5) to decompose Δ_i. In other words, we can write:

$$\Delta_i(y,z) = \sum_{i=1}^{M} v_{ji}\delta_j(y,z) \qquad (13)$$

where v_{ji} are unknown coefficients and M is the number of dry modes involved in this simplified approach.

The first step in the Rayleigh-Ritz method is to estimate the energy of the wet structure. According to Shames [8], the maximal deformation energy U may be evaluated from:

$$U = \frac{D}{2}\int_0^H\int_0^l\left(\left(\frac{\partial^2\Delta_i}{\partial y^2}\right)^2 + \left(\frac{\partial^2\Delta_i}{\partial z^2}\right)^2 + 2\nu\frac{\partial^2\Delta_i}{\partial y^2}\frac{\partial^2\Delta_i}{\partial z^2}\right.$$
$$\left. + 2(1-\nu)\left(\frac{\partial^2\Delta_i}{\partial y\partial z}\right)^2\right)\cdot dydz \qquad (14)$$

while the maximal kinetic energy T characterizing the vibrations of the plate is given by:

$$T = \frac{\Omega_i^2}{2}\rho t_p\int_0^H\int_0^l\Delta_i^2\cdot dydz \qquad (15)$$

In addition to U and T, it is also required to evaluate the potential W associated to the hydrodynamic flexible pressure p_f. This one may be shown to have the following form:

$$W = \frac{\Omega_i^2}{2}\sum_{n=1}^{+\infty}\sum_{m=0}^{+\infty}2\rho_f\frac{1-\cosh(\xi_{mn}L)}{\xi_{mn}h_s l_m\sinh(\xi_{mn}L)}I_{mn}^{(i)}I_{mn}^{(i)} \qquad (16)$$

where I_{mn} has already been defined in equation (12). If we further introduce (13) in (14), (15) and (16), it is clear that the terms U, T and W may be expressed as functions of v_{ji} and δ_j.

This operation is quite fastidious but allows us to write U, T and W under a more convenient matrix form. Indeed, we have:

$$T = \underline{v}_i^T\cdot[T]\cdot\underline{v}_i \quad U = \underline{v}_i^T\cdot[U]\cdot\underline{v}_i \quad W = \underline{v}_i^T\cdot[W]\cdot\underline{v}_i \qquad (17)$$

where $\underline{v}_i$ is a vector containing the coefficients v_{ji}. $[T]$, $[U]$ and $[W]$ are matrices that may be directly evaluated by considering the dry modes given by equation (5). Finally, solving the following classical eigenvalue problem:

$$\det\left([U]-\Omega_i^2([T]-[W])\right) = 0$$
$$\left([U]-\Omega_i^2([T]-[W])\right)\cdot\underline{v}_i = \underline{0} \qquad (18)$$

leads to the wet eigenfrequencies Ω_i and to the unknown coefficients v_{ji}. These last ones may then be introduced in (13) to get the wet mode shapes Δ_i.

4 NUMERICAL EVALUATION OF THE WET MODAL PROPERTIES

In order to validate the analytical developments briefly exposed in section 3, we can compare the corresponding results to those obtained by resorting to finite elements methods. As practical example, let us consider the reservoir depicted on Figure 3. It is characterized by a width of 7 m, a length of 15 m and a height of 6 m. It is filled with water up to a level of 3.5 m. The thickness t_p of the two flexible walls is equal to 10 cm.
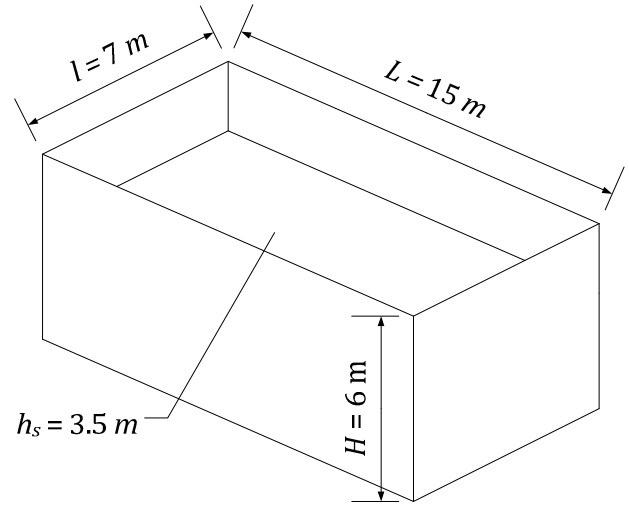

Figure 3. Main dimensions of the reservoir.

The physical properties defining the fluid and the solid are listed in Table 1. For this study, the reservoir is assumed to be made of steel.

Table 1. Properties for the fluid and the solid domains.

Solid domain		
Young modulus	E	210 GPa
Poisson coefficient	ν	0.3
Mass density	ρ	7890 kg/m^3
Fluid domain		
Bulk modulus	K_f	2.25 GPa
Speed of sound	c_f	1500 m/s
Mass density	ρ_f	1000 kg/m^3

The finite elements software NASTRAN is used to perform a modal analysis of the reservoir shown on Figure 3. The flexible walls are modeled by using isoparametric quadrilateral CQUAD shell elements with four grid points, while hexahedral CHEXA solid elements with eight grid points are used for the fluid. The mesh size has been progressively reduced until a sufficient convergence on the results was reached.

Working with NASTRAN allows us to know the modal properties of the wet flexible walls. These ones may be confronted to the results obtained by our simplified method. As a matter of comparison, let us start by considering the eigenfrequencies. The values found numerically and analytically are presented in Table 2 for the seventh first modes of vibration.

Table 2. Comparison of the eigenfrequencies

Mode number	Analytical solution (Hz)	Numerical solution (Hz)	Relative error (%)
1	5.44	5.43	0.22
2	12.51	12.36	1.12
3	18.27	18.27	0.01
4	26.52	26.12	1.53
5	32.79	32.37	1.28
6	39.44	39.44	0.01
7	48.37	47.21	2.49

From Table 2, we see that the maximal discrepancy between the results given by NASTRAN and the ones derived by the present simplified approach does not exceed 3%, which seems to be acceptable. Moreover, this quite good agreement was obtained by considering only five dry modes (i.e. $M = 5$) in equation (13).
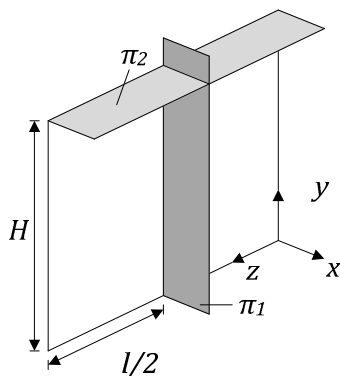

Figure 4. Vertical and horizontal planes π_1 and π_2 used for comparing the mode shapes.

Let us now compare the wet mode shapes obtained for the flexible walls of the reservoir. The two first ones are plotted on Figure 5 and Figure 6 respectively. For each mode, two different illustrations are proposed. The upper one is a plot of the profile in the vertical plane $z = l/2$ (plane π_1 on Figure 4), while the lower one corresponds to the profile in the horizontal plane $y = H$ (plane π_2 on Figure 4).

Regarding the horizontal profile, it is clear that a sine half-wave seems to be a good approximation. Concerning the vertical one, the agreement appears to be satisfactory, even if some discrepancy may be observed near the top of the gate where water is not present.
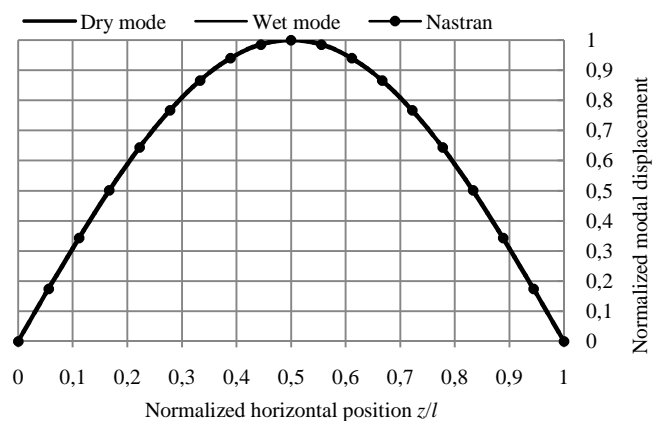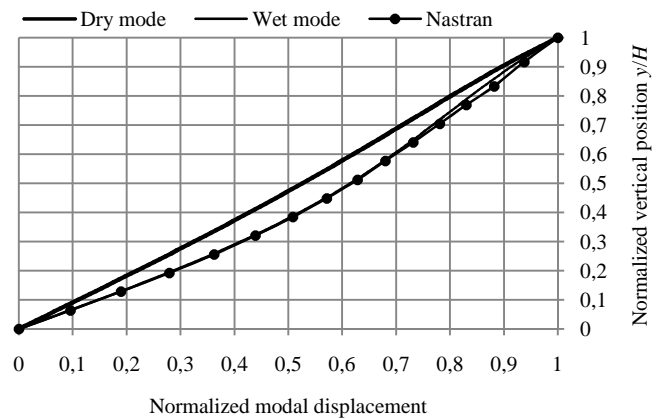

Figure 5. Comparison of the first mode shape in π_1 and π_2
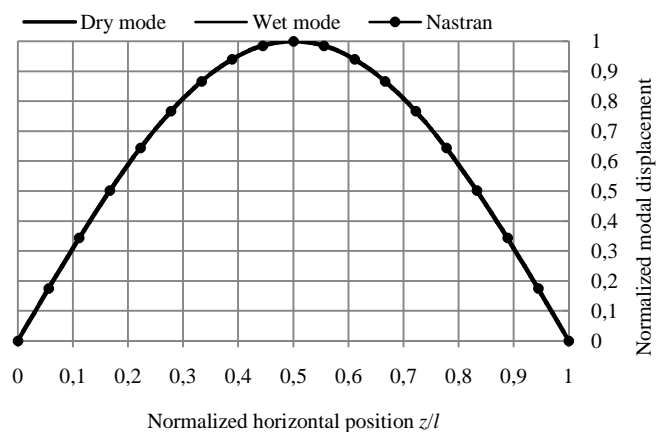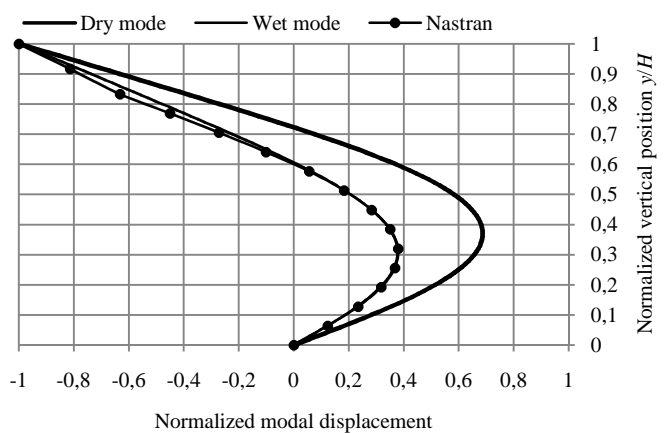

Figure 6. Comparison of the second mode shape in π_1 and π_2

The comparisons illustrated here above for this reservoir show that the agreement between the analytical and numerical results is satisfactory. This tends to validate the theoretical derivation of the vibration properties for an immerged plate by using the Rayleigh-Ritz method. The present analytical approach has also been corroborated by additional comparisons performed with other various reservoirs that are not presented here.

5 DYNAMIC ANALYSIS OF A WET PLATE

5.1 Equilibrium equation

The modal analysis of immerged flexible walls performed in the previous section provides a global insight on the way such structures respond to a seismic excitation. The next step is now to consider the situation where the reservoir is submitted to an earthquake load having a longitudinal acceleration component denoted by $\ddot{X}(t)$.

To get an analytical approximation of the dynamic response of the reservoir in such circumstances, we can refer to the equilibrium equation (1). Nevertheless, this one will be modified here to account for an eventual damping that may affect the structure. If we denote by f_d the damping forces, equation (1) becomes:

$$\rho t_p \left(\ddot{X} + \ddot{u} \right) + f_d + D\nabla^4 u = -p \tag{19}$$

In order to characterize a bit further the term f_d, we will assume that these additional forces are directly related to the velocity. Assuming a Rayleigh-type damping, f_d may be seen as having two different contributions: a first one coming from the mass of the structure and a second one coming from its stiffness. According to Shames [8], we can write:

$$f_d = \alpha \rho t_p \dot{u} + \beta D\nabla^4 \dot{u} \tag{20}$$

where α and β are two constants known as the Rayleigh damping coefficients. Furthermore, if we rearrange (19), we get:

$$D\nabla^4 u = -\left(p - \rho t_p \left(\ddot{X} + \ddot{u} \right) - \alpha \rho t_p \dot{u} + \beta D\nabla^4 \dot{u} \right) \tag{21}$$

which may be identified as the equilibrium equation of a plate submitted to an external resulting horizontal action f_{ext} given by the right hand side of (21). In fact, f_{ext} is nothing more than the sum of the pressure, damping and inertial forces. On the contrary, the left hand side of (21) may be seen as an internal force f_{int}.

5.2 Virtual work principle

Once all the forces acting on the structure have been characterized, we can try to derive analytically the forced vibrations of an immerged plate. To do so, a solution is to apply the virtual work principle, which simply states that a necessary and sufficient condition for equilibrium is to equate the external and internal virtual works for any kinematically compatible displacements field. Consequently, if we want to express the equilibrium of the plate, we first may consider a compatible virtual field $\delta u(y,z,t)$ acting on it.

Furthermore, if we consider the developments performed in section 3.3, it seems reasonable to express that the motions

$u(y,z,t)$ exhibited during the seismic excitation are based on the wet mode shapes. In other words, we postulate that:

$$u = \sum_{j=1}^{N} q_j(t)\Delta_j(y,z) \quad \delta u = \sum_{k=1}^{N} \delta q_k(t)\Delta_k(y,z) \tag{22}$$

where N is the number of wet modes used for developing $u(y,z,t)$. At this stage, the modal amplitudes q_j and δq_k are still unknown but will be determined by applying the virtual work principle.

5.3 Internal virtual work

During the virtual displacement δu, the work performed by the internal forces f_{int} is simply given by:

$$\delta W_{\text{int}} = \int_0^H \int_0^l f_{\text{int}} \cdot \delta u \cdot dydz = D \int_0^H \int_0^l \nabla^4 u \cdot \delta u \cdot dydz \tag{23}$$

which may be transformed by considering the modal decomposition (21). Doing so leads to an expression of δW_{int} involving the wet modes calculated in section 3.3:

$$\delta W_{\text{int}} = \sum_{k=1}^{N} \delta q_k \sum_{j=1}^{N} q_j U_{jk} \tag{24}$$

5.4 External virtual work

If we now develop the second part of the virtual work theorem, the work associated to the external forces during the virtual displacement $\delta u(y,z,t)$ is given by:

$$\delta W_{ext} = \int_0^H \int_0^l f_{ext} \cdot \delta u \cdot dydz \tag{25}$$

and subsequently, we have to examine the contributions coming from all the terms involved in the right hand side of (21). This task is quite fastidious, so we will only provide here a short summary of the final results, obtained after having incorporated the modal form (21) into (25). The following results can be easily proved (see also in the Appendix for more details):

- For the inertia forces, we get the following virtual work:

$$-\sum_{k=1}^{N} \delta q_k \left(\sum_{j=1}^{N} \ddot{q}_j T_{jk} + \ddot{X} \int_0^H \int_0^l \rho t_p \Delta_k dydz \right) \tag{26}$$

- For the Rayleigh damping forces, we get the following virtual work:

$$-\sum_{k=1}^{N} \delta q_k \sum_{j=1}^{N} \dot{q}_j \left(\alpha T_{jk} + \beta U_{jk} \right) \tag{27}$$

- For the pressure, we get the following virtual work:

$$-\sum_{k=1}^{N} \delta q_k \left(\int_0^H \int_0^l p_r \Delta_k dydz - \sum_{j=1}^{N} \ddot{q}_j W_{jk} \right) \tag{28}$$

5.5   Global equilibrium equation

If we gather all the results obtained in (24), (26), (27) and (28), we can write the virtual work principle in the following way:

$$\sum_{j=1}^{N} \ddot{q}_j \left(T_{jk} - W_{jk} \right) + \sum_{j=1}^{N} \dot{q}_j \left(\alpha T_{jk} + \beta U_{jk} \right) + \sum_{j=1}^{N} q_j U_{jk} \tag{29}$$
$$= V_k \ddot{X}$$

with $k = 1, 2, \ldots , N$. It is worth noting that the virtual coefficients δq_k do not appear anymore in (29) as the virtual work principle has to be satisfied for any value of these parameters. Furthermore, it is important to recall that T_{jk}, U_{jk}, W_{jk} and V_k may be directly expressed with help of the wet mode shapes. Some more detailed results are given in the Appendix.

As a final step, let us write (29) under a matrix form. If we introduce the matrices $[T]$, $[U]$, $[W]$ and the vectors $\underline{q}$ and $\underline{V}$, we can express (29) by the following more classical result:

$$\left([T] - [W] \right) \underline{\ddot{q}}(t) + \left(\alpha [T] + \beta [U] \right) \underline{\dot{q}}(t) + [U] \underline{q}(t) = \underline{V} \ddot{X}(t) \tag{30}$$

For a given acceleration $\ddot{X}(t)$, this equation may be solved by using the classical Newmark integration scheme for example. Doing so leads to the vector $\underline{q}$ containing the coefficients q_j. These ones are then used to derive the dynamic response of the flexible walls with help of equation (22).

6   NUMERICAL EVALUATION OF THE DYNAMIC RESPONSE

6.1   Description of the seismic action

To validate the analytical developments briefly exposed in section 5, we can compare them to those obtained by using a finite element model. The reservoir considered in section 4 (Figure 3), for which the material and fluid properties are those listed in Table 1, is submitted to a seism having the longitudinal acceleration $\ddot{X}(t)$ depicted on Figure 7.
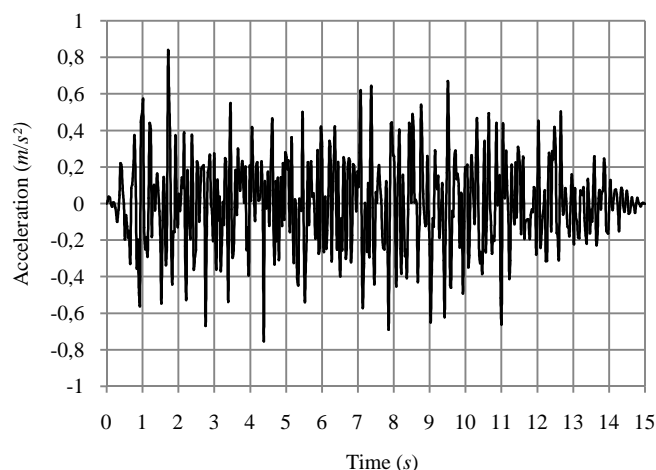

Figure 7. Longitudinal component of the seismic acceleration

The Fourier transform of this signal, represented on Figure 8, shows that the main part of the seismic excitation is located in the frequency range [1 *Hz* ; 15 *Hz*].
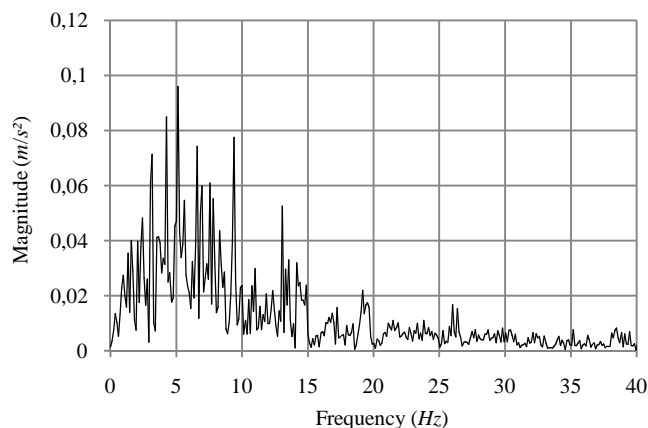

Figure 8. Fourier transform of the seismic acceleration

6.2   Description of the model

The numerical analysis is performed by using the finite elements software LS-DYNA. The flexible walls are modeled with Belytschko-Tsay shell elements [10] of uniform thickness t_p. The constitutive material is supposed to be elastic and characterized by a mass density ρ, a Young modulus E and a Poisson ratio v (see Table 1). The stress and strain tensors are related according to the classical Hooke's law.

The mesh of the solid domain is quite coarse, with a more or less regular size of 20×20 *cm* for the shell elements. This choice is due to the necessity of limiting the size of the model. Nevertheless, we also performed simulations on more refined models with a meshing of 5×5 *cm* or 10×10 *cm*, and the obtained results were not sensitively different from the present ones.

The fluid is modeled with constant stress solid elements [10] and supposed to behave like an elastic medium characterized by a mass density ρ_f and a bulk modulus K_f (see Table 1), but without shearing forces inside this material. This is coherent with the behavior of water.

The mesh of the fluid domain is also regular, with an approximate size of 19 *cm* for the solid elements. Here again, using more refined meshes does not change noticeably the results.

The both previous meshes representing the water and the structure do not share any node in common, which means that the fluid nodes are allowed to slide on the solid walls. A penalty contact algorithm is used to simulate the interaction between the plate and the surrounding liquid, which prevents the fluid from passing through the structure.

6.3   Presentation of the results

The analytical predictions derived from the virtual work principle are now confronted to the numerical ones. In this section, we will limit our presentation to the case of the reservoir depicted on Figure 3. Structural damping is applied on LS-DYNA through the classical Rayleigh formulation. The mass and stiffness coefficient are calibrated so as to model an arbitrary 4 % damping on the two first modes of vibration.

It is worth mentioning that many other additional simulations were performed, using different geometrical configurations than the one of Figure 4. The conclusions that we found in all cases are very similar to those presented here, so for conciseness, we will not present them in this paper.
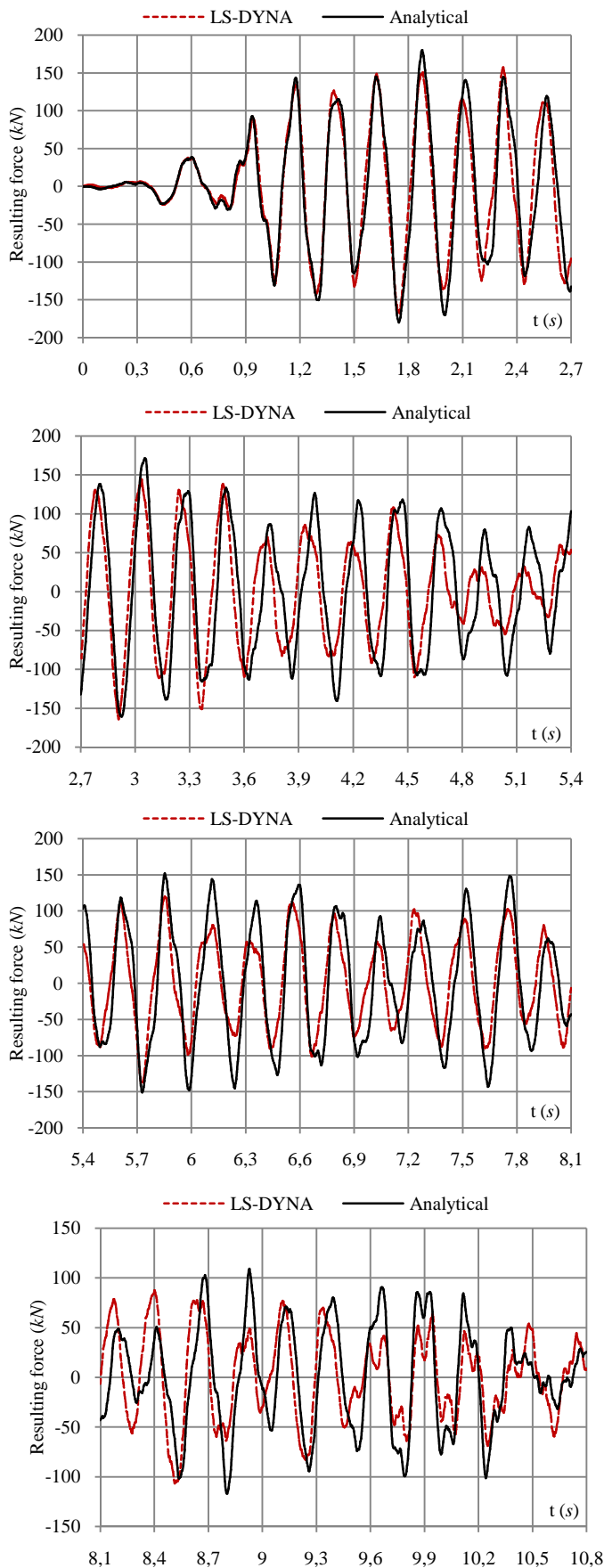
Figure 9. Comparison over four different time intervals

As matter of comparison between analytical and numerical results, we can compare the total hydrodynamic force $F(t)$ applied on the flexible wall (in excess to the hydrostatic pressure) is plotted on Figure 9 for different time intervals. As we neglect here the convective contribution, this resultant force is simply obtained by integrating the rigid and flexible impulsive pressures p_r and p_f over the wall surface.

We see that the agreement between analytical results and numerical ones is quite satisfactory. The comparison of the extreme values, extracted from the previous curves and listed in Table 3, shows that the theoretical model tends to be more conservative than the finite element one. Moreover, the maximal overestimation does not exceed 15 %, which is acceptable for a pre-design study. Analytical and numerical simulations performed for other reservoirs led to similar conclusions.

Table 3. Comparison of the extreme values

Result	Analytical solution (*kN*)	Numerical solution (*kN*)	Relative error (%)
Maximal value	180.09 kN	157.36 kN	14.4
Minimal value	-179.88 kN	-167.29 kN	7.5

7 CONCLUSION

In this paper, we briefly present an analytical procedure to analyze the dynamic response of flexible reservoirs submitted to an earthquake.

To achieve this goal, we first evaluate the wet modes characterizing the free vibrations of a plate in contact with water on one side. These modal properties are derived by using the Rayleigh-Ritz method. To check the validity of the results given by this approach, we compare them to numerical solutions obtained by using the finite elements software NASTRAN. These ones are derived by performing a modal analysis on a model where both the fluid and the solid are represented. For all the reservoirs tested, the agreement with the analytical results is found to be satisfactory.

As soon as the wet modal properties are derived, it is possible to have a better investigation of the dynamic response of a reservoir submitted to a seism. The virtual work principle is used to derive an analytical solution to the problem. This one is then validated by comparison with numerical results provided by the software LS-DYNA. Once again, a sufficient agreement is found between analytical and numercial results.

In comparison with numerical techniques, the main advantages of the present approach may be summarized in the following way:

- The method quickly provides the approximate time evolution of the total hydrodynamic pressure acting on a flexible wall for a given acceleration $\ddot{X}(t)$. This may be particularly useful during the early design stages of new structures, when engineers do not necessarily have time to resort to finite elements software.
- In comparison with numerical approaches, our simplified method has also the advantage of being quite intuitive. Indeed, using finite elements software is still quite arduous, as having a proper numerical representation of

the fluid-structure interaction is not that easy. This requires from engineers to be highly familiar with all the various modeling techniques, which is not necessarily always the case.

- Finally, we can also argue that the present simplified method is particularly well suited for working with important structures (such as lock chambers or large reservoirs). Indeed, such configurations may lead to very huge finite elements models requiring non negligible calculation times.

Even if this paper is only dealing with the seismic design of reservoirs, it constitutes a first step for developing a similar simplified tool applicable to lock gates. Indeed, the main difference between the reservoir considered here and a lock chamber is that the flexible walls have to be replaced by the lock gates. By following a similar analytical procedure, it should be therefore possible to derive the same kind of results for these particular structures. This will be precisely the goal of further investigations.

APPENDIX

This appendix provides a more detailed description of the formulae leading to the evaluation of the matrices $[T]$, $[U]$, and $[W]$ introduced in equation (30). These matrices are only functions of the wet eigenmodes of vibration. These last ones are given by (13) and may be derived by following the procedure described in section 3. As soon as they are found, they can be introduced in the following expressions:

$$T_{jk} = \rho t_p \int_0^H \int_0^l \Delta_j \Delta_k \, dy dz$$

$$U_{jk} = D \int_0^H \int_0^l \nabla^4 (\Delta_j) \Delta_k \, dy dz \tag{31}$$

$$W_{jk} = \sum_{n=1}^{+\infty} \sum_{m=0}^{+\infty} 2\rho_f \frac{1 - \cosh(\xi_{mn}L)}{\xi_{mn} h_s l_m \sinh(\xi_{mn}L)} I_{mn}^{(j)} I_{mn}^{(k)}$$

where I_{mn} has already been defined by equation (12). In addition, the various components of the vector $\underline{V}$ are to be found by applying the subsequent relation:

$$V_k = \int_0^{h_s} \int_0^l \left(\sum_{n=1}^{+\infty} \frac{4\rho_f}{\beta_n^2 L} \frac{\cosh(\beta_n y)}{\cosh(\beta_n h_s)} - \frac{L}{2} \right) \cdot \Delta_k \, dy dz$$
$$- \rho t_p \int_0^H \int_0^l \Delta_k \, dy dz \tag{32}$$

where $\beta_n = (2n-1)\pi/L$ and ρ_f is the mass density of the fluid, as mentioned previously.

REFERENCES

[1] H.I. Epstein, *Seismic design of liquid storage tanks*, Journal of the Structural Division, Vol. 102, No 9, pp.1659-1673, 1976.

[2] M.A. Haroun, *Stress analysis of rectangular walls under seismically induced hydrodynamic loads*, Bulletin of Seismological Society of America, Vol. 74, No. 3, pp. 1031-1041, 1984.

[3] G.W. Housner, *Dynamic pressures on accelerated fluid containers*, Bulletin of Seismological Society of America, Vol. 47, No. 1, pp. 15-37, 1957.

[4] R.A. Ibrahim, *Liquid sloshing dynamics: theory and applications*, Cambridge University Press, Cambridge, United Kingdom, 2005.

[5] A.W. Leissa, *The free vibration of rectangular plates*, Journal of Sound and Vibration, Vol. 31, No. 3, pp. 257-293, 1973.

[6] J.K. Kim, H.M. Koh, I.J. Kwahk, *Dynamic response of rectangular flexible fluid containers*, Journal of Engineering Mechanics, Vol. 122, No. 9, pp. 807-817, 1996.

[7] C. Rajalingham, R.B. Bhat, G.D. Xistris, *Vibration of rectangular plates using plate characteristic functions as shape functions in the Rayleigh-Ritz method*, Journal of Sound and Vibration, Vol. 193, No. 2, pp. 497-509, 1996.

[8] I.H. Shames, C.L. Dym, *Energy and finite element methods in structural mechanics*, New Age International Publishers, New Dehli, India, 1995.

[9] MSC Software, *MSC NASTRAN reference manual*, MSC Software Corporation, Santa Ana, United States, 2012.

[10] J.O. Hallquist, *LS-DYNA theoretical manual*, Livermore Software Technology Corporation, Livermore, United States, 2006.